Journal of Engineering Mathematics, Vol. 11, No. 1, January 1977
Noordhoff International Publishing–Leyden
Printed in The Netherlands

A two-dimensional model for the cochlea

II. The heuristic approach and numerical results

M. A. VIERGEVER

Department of Mathematics, Delft University of Technology, Delft, The Netherlands

(Received October 1, 1975)

SUMMARY

An alternative is given for the approach of the two-dimensional problem presented in [12]. Because of the mathematical simplicity of this alternative, several extensions of the model are possible. In this work the compressibility of the perilymph and variations of the scalaheight are considered; other extensions are briefly discussed.

The numerical calculations lead to the following conclusions: (1) the results of the one- and two-dimensional models show large quantitative but hardly any qualitative differences; (2) Von Békésy's [1] conclusions concerning the influence of the scalaheight upon the motion of the partition are incorrect; (3) the quantitative discrepancies between the model's results and the experiments of Rhode [6] can be eliminated by a large reduction of the scalaheight; (4) the phase difference as a function of frequency and the phase velocity show no qualitative disparities with the experimental data; (5) models with few sections, such as the hybrid computer model of Hubbard and Geisler [4] are inaccurate.

1. Introduction

In [12] a two-dimensional model for the cochlea was presented. The formulation of the problem as a boundary-value problem led to two coupled integral equations for the pressure difference across the windows and that across the membrane. By means of an asymptotic method an ordinary differential equation with boundary conditions could be obtained for the transmembrane pressure (i.e. the pressure difference across the membrane). This equation appeared to be an improvement of the corresponding equation resulting from one-dimensional models. An important feature of the model is the validity of the equation for all frequencies, so that no longer either a short-wave or a long-wave approximation is required.

It turns out to be possible to derive the same differential equation by a method which is more direct but somewhat less rigorous than the one used in [12]. The approach used in this work (Section 2) is not to be regarded in itself, since then the more rigorous method is preferable. The simplicity of the present approach enables us however to extend the model in various ways without making the computations too complicated. In Section 3 the compressibility of the fluid and variations in the scalaheight will be taken into account. Extension to a three-dimensional model and replacement of the membrane by a plate are briefly discussed. Furthermore attention will be paid to the viscosity of the perilymph.

In Section 4 the results of the numerical calculations will be shown. The difference between the one-dimensional and the two-dimensional models will be outlined; the in-

fluence of the scalaheight upon the motion of the partition and the influence of the discretization in the axial direction, which is necessary for the solution of the differential equation, also are looked upon.

In Section 5 the results are discussed and compared with experimental data and with results of other models. Some interesting conclusions can be drawn.

2. The heuristic method

As a starting point the same assumptions as in [12] are used. These were:
- only linear phenomena are considered; the driving forces and the resulting responses are taken to be so small that non-linear effects are excluded,
- the spiral coiling is dispensed with,
- the scala media is replaced by a single membrane,
- variations in the direction along the width of the membrane are ignored,
- the scala walls are rigid,
- the heights of the scalae are equal and constant,
- the fluid is considered as incompressible and inviscid.

One simplification, viz. the extension of the membrane to infinity, is omitted. Now the cochlea can be represented by Fig. 1.

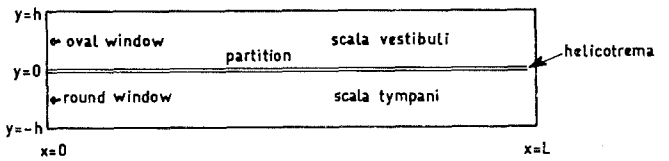

Figure 1.

The scale of this figure is not correct; in reality $h \simeq 0.1$ cm, while $L \simeq 3.5$ cm.

Let $\tilde{p}_{sv}(x, y; t)$ be the pressure in the scala vestibuli and $\tilde{p}_{st}(x, y; t)$ the pressure in the scala tympani. Then the difference pressure $\tilde{P}(x, y; t)$ can be defined by

$$\tilde{P}(x, y; t) = \tilde{p}_{st}(x, -y; t) - \tilde{p}_{sv}(x, y; t), \qquad y > 0. \tag{2.1}$$

Only harmonic oscillations are considered with period $2\pi/\omega$; then it holds that

$$\tilde{P}(x, y; t) = P(x, y)e^{i\omega t}. \tag{2.2}$$

It can be proved easily [12] that $P(x, y)$ satisfies Laplace's equation

$$P_{xx}(x, y) + P_{yy}(x, y) = 0. \tag{2.3}$$

Subscripts denote differentiation with respect to the variable involved. Two of the four boundary conditions for (2.3) are specified. The first is

$$P_y(x, h) = 0, \tag{2.4}$$

which follows from the vanishing of the y-component of the fluid velocity on the walls $y = h$ and $y = -h$. The second condition is a relation between the transmembrane pressure

and the velocity of the membrane:

$$2P(x, 0) + \zeta(x)P_y(x, 0) = 0. \tag{2.5}$$

The impedance $\zeta(x)$ of the cochlear partition is expressed in the point-wise mechanical properties of the membrane as follows:

$$\zeta(x) = (c - m\omega^2 + ik\omega)/(\rho\omega^2), \tag{2.6}$$

with $m(x)$, $k(x)$ and $c(x)$ mass, resistance and stiffness of the membrane per unit area and ρ the density of the fluid.

The other two boundary conditions, one at $x = 0$ and one at $x = L$, are as yet irrelevant.

Since the height of a scala is small compared to its length (the ratio is approximately 1/35), $P(x, y)$ is expanded in a Taylor series around the partition; the remainder has the Lagrange form.

$$P(x, y) = \sum_{n=0}^{N+1} \frac{y^n}{n!} \frac{\partial^n}{\partial y^n} P(x, 0) + \frac{y^{N+2}}{(N+2)!} \frac{\partial^{N+2}}{\partial y^{N+2}} P(x, \theta y), \qquad 0 < \theta < 1. \tag{2.7}$$

In view of the sequel, $P(x, y)$ is required to be $N + 3$ times continuously differentiable with respect to x and $N + 2$ times with respect to y. When this condition is satisfied, the expansion as in (2.7) is justified. It is assumed that the remainder term of the series in (2.7) can be neglected because of the small values of y ($y \leqq h$; $h \simeq 0.1$ cm), provided that N is large enough. It follows that

$$P(x, y) = \sum_{n=0}^{N+1} \frac{y^n}{n!} \frac{\partial^n}{\partial y^n} P(x, 0). \tag{2.8}$$

With the help of (2.8) eq. (2.4) yields:

$$\sum_{n=0}^{N} \frac{h^n}{n!} \frac{\partial^{n+1}}{\partial y^{n+1}} P(x, 0) = 0. \tag{2.9}$$

Equation (2.5) remains unaltered, but eq. (2.3) changes into

$$\sum_{n=0}^{N-1} \frac{y^n}{n!} \left(\frac{\partial^{n+2}}{\partial x^2 \partial y^n} + \frac{\partial^{n+2}}{\partial y^{n+2}} \right) P(x, 0) + \sum_{n=N}^{N+1} \frac{y^n}{n!} \frac{\partial^{n+2}}{\partial x^2 \partial y^n} P(x, 0) = 0. \tag{2.10}$$

This relation must hold for all values of y, so that

$$\left(\frac{\partial^{n+2}}{\partial x^2 \partial y^n} + \frac{\partial^{n+2}}{\partial y^{n+2}} \right) P(x, 0) = 0, \qquad 0 \leqq n \leqq N - 1. \tag{2.11}$$

Hence the partial derivatives of $P(x, y)$ with respect to y can be expressed in those with respect to x. For y-derivatives of even order it is found that

$$\frac{\partial^{2n+2}}{\partial y^{2n+2}} P(x, 0) = (-1)^{n+1} \frac{\partial^{2n+2}}{\partial x^{2n+2}} P(x, 0), \qquad 0 \leqq n \leqq (N - 1)/2. \tag{2.12}$$

and for those of odd order, using (2.5), that

$$\frac{\partial^{2n+1}}{\partial y^{2n+1}} P(x, 0) = (-1)^n \frac{\partial^{2n+1}}{\partial y \partial x^{2n}} P(x, 0) = (-1)^{n+1} \frac{\partial^{2n}}{\partial x^{2n}} \left\{ \frac{2P(x, 0)}{\zeta(x)} \right\}, \qquad 0 \leqq n \leqq N/2. \tag{2.13}$$

Insertion of (2.12) and (2.13) into (2.9) leads to

$$\sum_{n=0}^{N/2} (-1)^{n+1} \frac{h^{2n}}{(2n)!} \frac{d^{2n}}{dx^{2n}} \left\{ \frac{2p(x)}{\zeta(x)} \right\} + \sum_{n=0}^{(N-1)/2} (-1)^{n+1} \frac{h^{2n+1}}{(2n+1)!} \frac{d^{2n+2}}{dx^{2n+2}} p(x) = 0. \tag{2.14}$$

For reasons of notation the transmembrane pressure $P(x, 0)$ is written as $p(x)$. The left hand side of (2.14) is actually a mixed series in $p(x)$ and $p(x)/\zeta(x)$. The mixed character causes difficulties in choosing N, since the error made with any choice of N has approximately the same order of magnitude as one of the terms in the remaining equation. The reason for this idle accuracy is the large interval of values of $|\zeta|$. For the range of hearing and with the use of the numerical values of Peterson and Bogert [5, 2] it can be calculated that $|\zeta|$ varies from less than 0.1 cm to more than 10^5 cm. The idle accuracy that occurs is illustrated by two examples. viz. $N = 1$ and $N = 2$. The resulting equations are respectively

$$hp_{xx} + \frac{2p}{\zeta} = 0, \tag{2.15}$$

$$hp_{xx} + \frac{2p}{\zeta} - h^2(p/\zeta)_{xx} = 0. \tag{2.16}$$

In (2.15) the first neglected term on the left hand side is $-h^2(p/\zeta)_{xx}$. For small values of $|\zeta|$ this will be of the same order of magnitude as hp_{xx}. In (2.16) the first neglected term is $-h^3 p_{xxxx}$. For large values of $|\zeta|$ the magnitude of this term will be the same as or even larger than $-h^2(p/\zeta)_{xx}$. It is possible to dispense with this idleness.

Choose $N = 3$; then (2.14) becomes

$$hp_{xx} - \frac{h^3}{6} p_{xxxx} + \frac{2p}{\zeta} - h^2(p/\zeta)_{xx} = 0. \tag{2.17}$$

The largest neglected terms are

$$\frac{h^5}{120} \frac{d^6 p}{dx^6} \text{ and } \frac{h^4}{12} \frac{d^4(p/\zeta)}{dx^4}.$$

The notation with subscripts is not used on account of the large number of differentiations. Differentiate (2.17) twice with respect to x and multiply all terms of the resulting equation with $h^2/6$. It follows that

$$\frac{h^3}{6} \frac{d^4 p}{dx^4} - \frac{h^5}{36} \frac{d^6 p}{dx^6} + \frac{h^2}{3} \frac{d^2(p/\zeta)}{dx^2} - \frac{h^4}{6} \frac{d^4(p/\zeta)}{dx^4} = 0. \tag{2.18}$$

Now substitute (2.18) into (2.17) and neglect the terms

$$-\frac{h^5}{36} \frac{d^6 p}{dx^6} \text{ and } -\frac{h^4}{6} \frac{d^4(p/\zeta)}{dx^4},$$

since these have the same order of magnitude as the largest neglected terms due to the truncation at $N = 3$. Then one finds

$$hp_{xx} + 2(p/\zeta) - \tfrac{2}{3}h^2(p/\zeta)_{xx} = 0. \tag{2.19}$$

It seems reasonable to set that the error due to truncation is small with respect to the left hand side terms of (2.19), independent of the value of ζ. At least it is clear that an idle accuracy as mentioned before is no longer present.

Equation (2.19) is the same equation as found in [12]. It remains to be proved that the boundary conditions are the same in the two models. For the condition at the helicotrema ($x = L$) this is clear at once, since there the pressure difference between the scalae is equalized. For harmonic oscillations this means that

$$p(L) = 0. \tag{2.20}$$

In [12] the cochlea was extended to infinity, but this is not necessary in the present model.

For the condition at the windows ($x = 0$), assume that $P(0, y)$ is prescribed. It is not correct to use $p(0) = P(0, 0)$ as a boundary condition for (2.19), since then the condition of the two-dimensional problem would be satisfied only for $y = 0$. To obtain a condition in terms of $P(0, y)$, $\overline{P(0, y)}$ is computed directly from (2.8):

$$\overline{P(0, y)} = h^{-1} \int_{y=0}^{h} P(0, y)\, dy = \sum_{n=0}^{N+1} \frac{h^n}{(n+1)!} \frac{\partial^n}{\partial y^n} P(0, 0). \tag{2.21}$$

Using (2.12) and (2.13) one gets

$$\overline{P(0, y)} = \sum_{n=0}^{(N+1)/2} \frac{(-1)^n h^{2n}}{(2n+1)!} \frac{\partial^{2n}}{\partial x^{2n}} P(0, 0) + 2 \sum_{n=0}^{N/2} \frac{(-1)^{n+1} h^{2n+1}}{(2n+2)!} \frac{d^{2n}}{dx^{2n}} w(0), \tag{2.22}$$

where $w(x) = P(x, 0)/\zeta(x)$.

Obviously N must have the same value as in the derivation of (2.19), viz. $N = 3$. Then (2.22) becomes

$$\overline{P(0, y)} = p(0) - hw(0) - \frac{h^2}{6} p_{xx}(0) + \frac{h^3}{12} w_{xx}(0) + \frac{h^4}{120} p_{xxxx}(0). \tag{2.23}$$

Once more $p(x)$ is used instead of $P(x, 0)$ since the y-dependence of $P(x, y)$ has been eliminated.

The largest neglected terms in (2.23) are $-h^6 p^{\mathrm{vi}}(0)/5040$ and $-h^5 w^{\mathrm{iv}}(0)/360$.

According to (2.19)

$$-\frac{h^2}{6} p_{xx}(0) = \frac{h}{3} w(0) - \frac{h^3}{9} w_{xx}(0), \quad w_{xx}(0) = -\frac{h}{2} p_{xxxx}(0) + \frac{h^2}{3} w_{xxxx}(0). \tag{2.24}$$

Substitution of (2.24) into (2.23) yields

$$\overline{P(0, y)} = p(0) - \frac{2h}{3} w(0) + \frac{h^4}{45} p_{xxxx}(0) - \frac{h^5}{108} w_{xxxx}(0). \tag{2.25}$$

The last term of (2.25) can be neglected since it has the same order of magnitude as one of the neglected terms in (2.23). Then still the condition found has a higher accuracy than the differential equation itself. For, the largest neglected terms in (2.17) have an order of magnitude which is $h^4 d^4/dx^4$ times that of the largest retained terms. With the same degree of accuracy, (2.25) becomes

$$p(0) = \frac{\overline{P(0, y)}}{1 - 2h/(3\zeta(0))}, \tag{2.26}$$

just as in [12].

Now the condition for the ordinary differential equation has been expressed as a function of the original condition for the two-dimensional problem. Only the magnitude, not the form of the prescribed difference pressure is of importance as to the motion of the partition. Therefore the model will not be described correctly by (2.19) with (2.20) and (2.26) in the immediate vicinity of the windows, since there the form of the input signal has its influence upon the flow and hence upon the motion of the membrane.

The mathematical treatment presented in the foregoing has been somewhat less rigorous than the one described in the first part of this work; this holds especially for the determination of the boundary condition at the windows. Moreover the choice of N has not been justified. We will return to this point in Section 3 where the effect of increasing the value of N is treated. The correctness of the mathematical description is hardly open to doubt, since the results are identical to those in [12]. On the other hand the model itself has many imperfections. These have to be removed as much as possible. In the next section several extensions of the present model are discussed utilizing the approach described above. Application of the method of part I to these extensions is not feasible.

3. Extensions of the model

The model of Section 2 can be extended easily in several ways because of its mathematical simplicity. In this work the compressibility of the perilymph and variations in the scalaheight are considered; the viscosity of the fluid is taken into account too, albeit in a different manner. Other extensions will be discussed shortly. Moreover attention is paid to more accurate differential equations than the one obtained in Section 2, by choosing a value of N larger than 3.

To start with the last, by choosing $N = 5$ and proceeding in the same way as in Section 2, one can derive that

$$hp_{xx} + \frac{2p}{\zeta} - \frac{2h^2}{3}(p/\zeta)_{xx} - \frac{2h^4}{45}(p/\zeta)_{xxxx} = 0. \tag{3.1}$$

This is a fourth order differential equation which needs four boundary conditions to be solved. One condition is (2.20), the second is the analogue of (2.26) for $N = 5$, the third and fourth conditions can be obtained from higher moments of $P(0, y)$, for example $\int_{y=0}^{h} yP(0, y)dy$ and $\int_{y=0}^{h} y^2P(0, y)dy$. Not only the determination of the boundary conditions, but also the numerical calculations become more complicated. Now consider the gain in accuracy that can be expected with respect to the truncation at $N = 3$. This gain should come from the last left hand side term. The numerical solution of (2.19) shows that the magnitude of this term is only a few percent of the magnitude of $2p/\zeta$. The argument used is somewhat tricky, since the crucial term was not taken along in the numerical calculations.

One remark must be made: the choice $N = 4$ would be a bad one, since then also a fourth order differential equation would result with the same disadvantages as (3.1), but a smaller

gain in accuracy, if any. Resuming it seems reasonable to conclude that $N = 3$ is the optimal value for our purpose. The next to be regarded is the compressibility of the perilymph. As a consequence of this, Laplace's equation (2.3) changes into

$$\Delta P(x, y) + \omega^2 P(x, y)/a^2 = 0, \tag{3.2}$$

where $\omega/2\pi$ is the frequency of the input signal and $a(\rho)$ the velocity of sound in the fluid; the latter is approximately a constant on account of the small variations in ρ. Naturally, eq. (2.10) changes likewise into

$$\sum_{n=0}^{N+1} \frac{y^n}{n!}\left(\frac{\partial^{n+2}}{\partial x^2 \partial y^n} + \frac{\omega^2}{a^2}\frac{\partial^n}{\partial y^n}\right)P(x, 0) + \sum_{n=0}^{N-1} \frac{y^n}{n!}\frac{\partial^{n+2}}{\partial y^{n+2}} P(x, 0) = 0. \tag{3.3}$$

The analogues for (2.12) and (2.13) then become

$$\frac{\partial^{2n+2}}{\partial y^{2n+2}} P(x, 0) = (-1)^{n+1}\left(\frac{\partial^2}{\partial x^2} + \frac{\omega^2}{a^2}\right)^{n+1} P(x, 0), \tag{3.4}$$

$$\frac{\partial^{2n+1}}{\partial y^{2n+1}} P(x, 0) = (-1)^{n+1}\left(\frac{\partial^2}{\partial x^2} + \frac{\omega^2}{a^2}\right)^{n}\left\{\frac{2P(x, 0)}{\zeta(x)}\right\}. \tag{3.5}$$

Substitution of (3.4) and (3.5) into (2.9) leads to

$$\sum_{n=0}^{N/2} (-1)^{n+1} \frac{h^{2n}}{(2n)!}\left(\frac{d^2}{dx^2} + \frac{\omega^2}{a^2}\right)^n \left\{\frac{2p(x)}{\zeta(x)}\right\} + \\ + \sum_{n=0}^{(N-1)/2} (-1)^{n+1} \frac{h^{2n+1}}{(2n+1)!}\left(\frac{d^2}{dx^2} + \frac{\omega^2}{a^2}\right)^{n+1} p(x) = 0. \tag{3.6}$$

For the range of hearing, $\omega < 10^5$ c.p.s. while $a = 1.43 * 10^5$ cm/s ([5]). Since $h \simeq 0.1$ cm, the dimensionless quantity $h^2\omega^2/a^2 < 0.01$, so that it can be ignored with respect to unity. Now with $N = 3$, (3.6) becomes

$$h\frac{\omega^2}{a^2} p + hp_{xx} - \frac{h^3}{6} p_{xxxx} + \frac{2p}{\zeta} - h^2(p/\zeta)_{xx} = 0. \tag{3.7}$$

With the process utilized in Section 2, this yields

$$hp_{xx} + h\frac{\omega^2}{a^2} p + \frac{2p}{\zeta} - \frac{2h^2}{3}(p/\zeta)_{xx} = 0. \tag{3.8}$$

With the same neglects the boundary conditions (2.20) and (2.26) remain unchanged.

The variation of the scalaheights with the axial coordinate x can be treated also with the heuristic method. The heights of the scalae are still considered as equal, since otherwise the difference pressure $P(x, y)$ could not be defined in such a simple way.

When $h = h(x)$, equation (2.4) is no longer valid. The vanishing of the normal component of the fluid velocity on the walls is now given by

$$-h_x P_x(x, h) + P_y(x, h) = 0, \tag{3.9}$$

which renders

$$\sum_{n=0}^{N} \frac{h^n}{n!} \frac{\partial^{n+1}}{\partial y^{n+1}} P(x, 0) - h_x \sum_{n=0}^{N+1} \frac{h^n}{n!} \frac{\partial^n}{\partial y^n} P_x(x, 0) = 0. \tag{3.10}$$

Substitution of (3.4) and (3.5) into (3.10) yields

$$\begin{aligned} &2 \sum_{n=0}^{N/2} (-1)^{n+1} \frac{h^{2n}}{(2n)!} \left(\frac{d^2}{dx^2} + \frac{\omega^2}{a^2} \right)^n (p/\zeta) + \\ &+ \sum_{n=0}^{(N-1)/2} (-1)^{n+1} \frac{h^{2n+1}}{(2n+1)!} \left(\frac{d^2}{dx^2} + \frac{\omega^2}{a^2} \right)^{n+1} p + \\ &- h_x \sum_{n=0}^{(N+1)/2} (-1)^n \frac{h^{2n}}{(2n)!} \left(\frac{d^2}{dx^2} + \frac{\omega^2}{a^2} \right)^n p_x - 2h_x \sum_{n=0}^{N/2} (-1)^{n+1} \times \\ &\times \frac{h^{2n+1}}{(2n+1)!} \left(\frac{d^2}{dx^2} + \frac{\omega^2}{a^2} \right)^n (p/\zeta)_x = 0. \end{aligned} \tag{3.11}$$

Application of the process used in Section 2 leads for $N = 3$ to a very complicated equation, even when $h^2\omega^2/a^2$ is ignored with respect to unity. Therefore a further simplification is made. From Zwislocki [14], it appears that $h(x)$ varies slowly from about 2 mm at the windows to 0.5 mm near the helicotrema. Hence the derivatives of $h(x)$ will have at most the same order of magnitude as $h(x)$ itself, say $O(h)$. Now $O(h^2)$ is neglected with respect to $O(1)$; the error made by this simplification can be a few percent only, which is negligible compared to the accuracy of the numerical data. Doing so, one finds after some tedious calculations, that (3.11) is approximated by

$$hp_{xx} + h_x p_x + h \frac{\omega^2}{a^2} p + \frac{2p}{\zeta} - 2hh_x(p/\zeta)_x - \tfrac{2}{3}h^2(p/\zeta)_{xx} = 0. \tag{3.12}$$

For this equation boundary condition (2.20) obviously still holds good. Condition (2.26) on the other hand must be replaced by another condition. With an analogous derivation as was used for (2.26) and neglecting once more $h^2\omega^2/a^2$ and $O(h^2)$ with respect to unity, one gets

$$\left\{ 1 - \frac{2h(0)}{3\zeta(0)} \right\} p(0) + \tfrac{1}{6}h(0)h_x(0)p_x(0) = \overline{P(0, y)}, \tag{3.13}$$

so that here also the conditions for the ordinary differential equation can be derived from the conditions of the two-dimensional model directly.

The viscosity of the perilymph can be taken into account by localizing the viscous effects in a boundary layer along the walls and the partition; the flow outside the layer is inviscid. When the problem is formulated in this way, the boundary layer quantities can be derived as functions of the main flow quantities and hence as functions of the solution of the inviscid problem. In [10] this was done for small driving forces, so that only linear effects are considered. In [9, 11] a correction was given for non-linear phenomena. The derivations were not confined to a one-dimensional treatment, so that the results can be applied to the present model.

Even with the above extensions, the model is still far from perfect. The main imperfection is the characterization of the cochlear partition by a point impedance function as in (2.5). Von Békésy [1] has shown that the basilar membrane has no significant tension and therefore is better represented by a plate, with a beam as analogue in the two-dimensional model. Then however the arches of Corti, which are stiff relative to the basilar membrane, are not taken into account. Hence a more detailed structure is necessary, as indicated by Steele [8]. With this representation no two-dimensional analogue can be found; the third direction is essential in the concept. Steele needed a rather specific geometry and some not justified mathematical simplifications besides to solve the three-dimensional problem. Because of its simplicity the heuristic approach enables a more general treatment; this however is preserved for a later paper.

4. Numerical results

To get an insight in the meaning of the results of the two-dimensional model, eq. (2.19) has been solved with the aid of a digital computer. For the sake of clarity the effects caused by compressibility of the fluid and by variations in the scala height were not taken into account. As boundary conditions for (2.19) were chosen $p(0) = 1$ dyn/cm^2 and $p(3.5) = 0$ dyn/cm^2. It is emphasized that this does not affect the two-dimensional character of the model. For, $p(0)$ depends on the average of $P(0, y)$ over y, so that only the magnitude of the input signal is of importance for the motion of the membrane; the form of the signal is irrelevant. The same conclusion was reached by Van Dijk [3]. To enable a comparison with one-dimensional models, equation (2.15) was also solved numerically. For, eq. (2.15) is identical to the Peterson–Bogert [5] equation for a cochlea with constant scala heights and an incompressible perilymph. It can be derived easily that the boundary condition at the windows is given by

$$p(0) = \overline{P(0, y)}, \tag{4.1}$$

so that, in agreement with the chosen conditions for (2.19), the boundary conditions for (2.15) are $p(0) = 1 - 2h/(3\zeta(0))$ dyn/cm^2 and $p(3.5) = 0$ dyn/cm^2. It is clear that (2.19) is equal to (2.15) plus a correction term, and that (2.26) can be written as (4.1) plus a correction term. The magnitudes of these correction terms are decisive for the difference between the motion of the partition in the one-dimensional and that in the two-dimensional model. Naturally the fluid motion is better represented by the two-dimensional model, since it has been shown by several workers that the assumption of uniformity of the pressure over a cross-section of a scala holds good only for small frequencies.

We are interested above all in the motion of the membrane. Let $\eta(x)$ be the displacement of the membrane. Then from (2.5) and the equation of motion it follows that:

$$\eta(x) = \frac{p(x)}{\rho\omega^2\zeta(x)}. \tag{4.2}$$

Hence $\eta(x)$ can be computed when (2.19) c.q. (2.15) is solved.

For the numerical integration of the differential equation a discretization of the x-interval $[0, L]$ was necessary. To this end the membrane was divided longitudinally in a number

of sections. This number was chosen to be 175 unless otherwise indicated; it will be shown that this choice is reasonable. The step unit in the integration process was consequently $3.5/175 = 0.02$ cm. Further the value of h was 0.1 cm; later in this section the effect of a different choice for h will be discussed. For $\zeta(x)$ the values introduced by Peterson and Bogert were taken, viz.

$$c(x) = 1.72 * 10^9 e^{-2x} \text{ dyn/cm}^3,$$

$$k(x) = 6.737 * 10^3 e^{-x} \text{ dyn.sec/cm}^3,$$

$$m(x) = 0.143 \text{ g/cm}^2,$$

while $\rho = 1.034$ g/cm^3, according to Von Békésy [1].

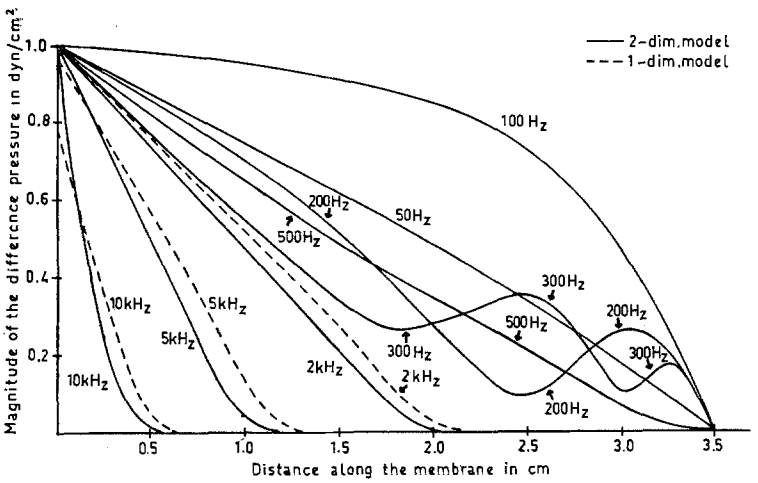

Figure 2. Magnitude of the difference pressure $p(x)$ as a function of the distance to the windows for various frequencies $\omega/2\pi$ of the input signal. In all cases $p(0) = 1$ dyn/cm^2. Comparable results of the 1-dimensional model are also shown; for frequencies $\leqq 500$ Hz the difference between the two models was relatively small.

In Fig. 2 a plot is shown of the magnitude of $p(x)$ for various frequencies in the range of hearing. It appears that, when $\omega/2\pi > 500$ Hz, $|p|$ decreases monotonically with x; the value of $|p|$ becomes negligible for a value of x that depends on the frequency. For frequencies between 100 and 500 Hz the travelling pressure wave reaches the helicotrema and reflects, whence standing waves appear. For frequencies under 100 Hz the whole membrane vibrates. The values of 100 and 500 Hz are of course strongly dependent on the chosen numerical values, especially on those of the mechanical properties of the membrane. The corresponding results of the one-dimensional model are shown for three frequencies, all with $p(0) = 1 - 2h/(3\zeta(0))$. One can see that the second right hand side term of this boundary condition is negligible for frequencies $\leqq 2$ kHz. The error caused by the one-dimensional concept can be considerable when one regards fixed values of x; yet structural disparities between the curves obtained from the two models are hardly discernable. For frequencies between 100 and 500 Hz the differences were small, and for frequencies under 100 Hz negligible.

In Fig. 3 the normalized amplitude of $\eta(x)$ is presented for several frequencies. The

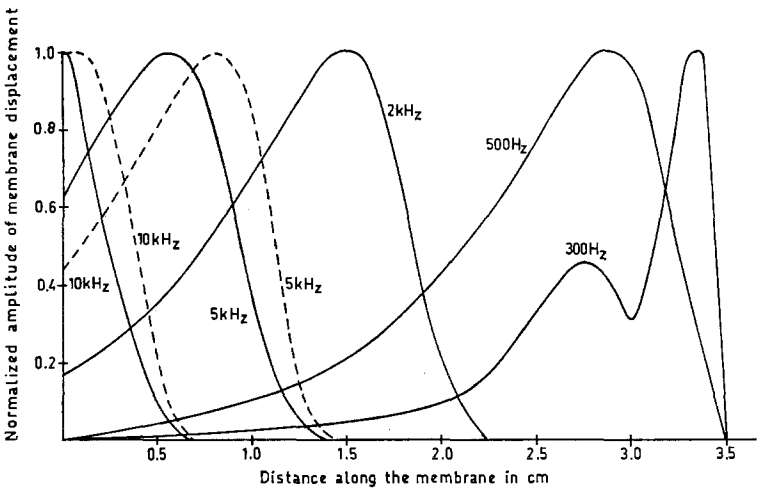

Figure 3. Normalized amplitude of the membrane displacement as a function of position on the membrane for various frequencies. Comparable results of the one-dimensional model are also shown for 5 and 10 kHz.

normalization is such that the value of the maximum is 1.0 for each frequency. A single maximum occurs for frequencies over 500 Hz; the position of the maximum varies with frequency. More than one local maximum is found when $100 < \omega/2\pi < 500$ Hz. For low frequencies (< 100 Hz), there is again only one maximum. Comparable data from the one-dimensional model show that for high frequencies the peaks of the curves are found at positions along the membrane different from those obtained by the two-dimensional model; the shapes of the curves on the contrary are similar. For low frequencies the differences were small.

The value of the largest deflection varies considerably with frequency when the input transmembrane pressure is kept constant. With $p(0) = 1$ dyn/cm^2, the maximum deflection

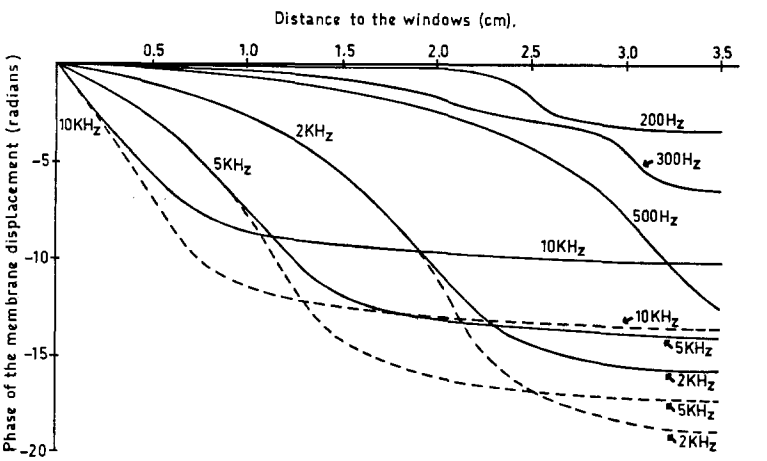

Figure 4. Phase of the membrane displacement $\eta(x)$ as a function of position along the membrane for various frequencies. Comparable results for the one-dimensional model are shown for 2,5 and 10 kHz. For frequencies $\leqq$ 500 Hz the difference between the two models was negligible. The phase was referenced to $\eta(0)$.

is roughly $8 * 10^{-10}$ cm for high frequencies (between 7 and 10 kHz) and more than $1 * 10^{-7}$ cm for 100 Hz.

Fig. 4 shows the phase of the membrane displacement with respect to distance for different frequencies. For frequencies < 100 Hz the phase lag is negligible so that the whole membrane practically moves in phase. The differences between the one- and two-dimensional models are deceptive, since the values of the two-dimensional model strongly depend on the value of h, the scala height; this is illustrated in the sequel. The phase of $p(x)$ is not presented; its picture is very similar to that of Fig. 4.

Fig. 5 compares transmembrane pressures for several scala heights at an input frequency of 1 kHz. The differences from the curve obtained using $h = 0.1$ cm are small, since this curve lies in between the two plotted curves for $h = 0.03$ cm and $h = 0.2$ cm.

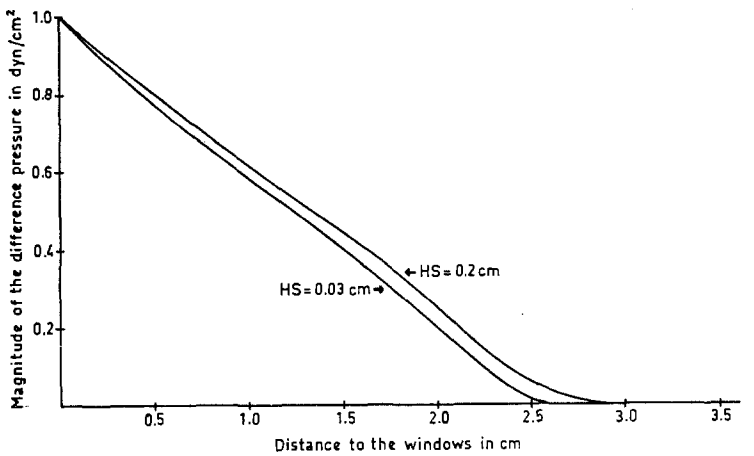

Figure 5. Magnitude of the difference pressure $p(x)$ as a function of position along the membrane for various scalaheights (HS). The frequency of the input signal was 1 kHz.

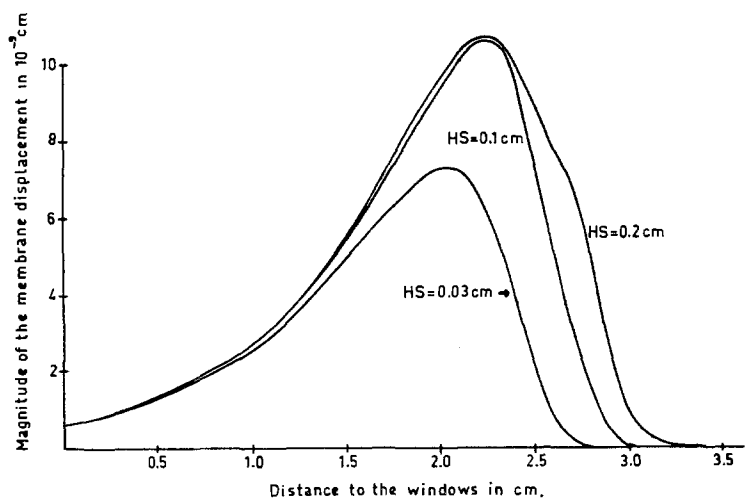

Figure 6. Magnitude of the membrane displacement $\eta(x)$ as a function of position along the membrane for various scalaheights (HS). Frequency of the input signal was 1 kHz.

The differences are larger for the magnitude of the membrane displacement, as appears from Fig. 6. Comparing $h = 0.1$ cm and $h = 0.2$ cm, one sees that the peaks are at the same position and have the same size; only the shape of the curves is somewhat different. The peak of the 0.03 cm curve however, is both smaller and closer to the basal end than that of the 0.1 cm curve.

The differences become still more pronounced when the phase of the membrane displacement is looked upon (Fig. 7). The phase of the transmembrane pressure gives the same picture. These results allow some interesting conclusions; they are presented in Section 5.

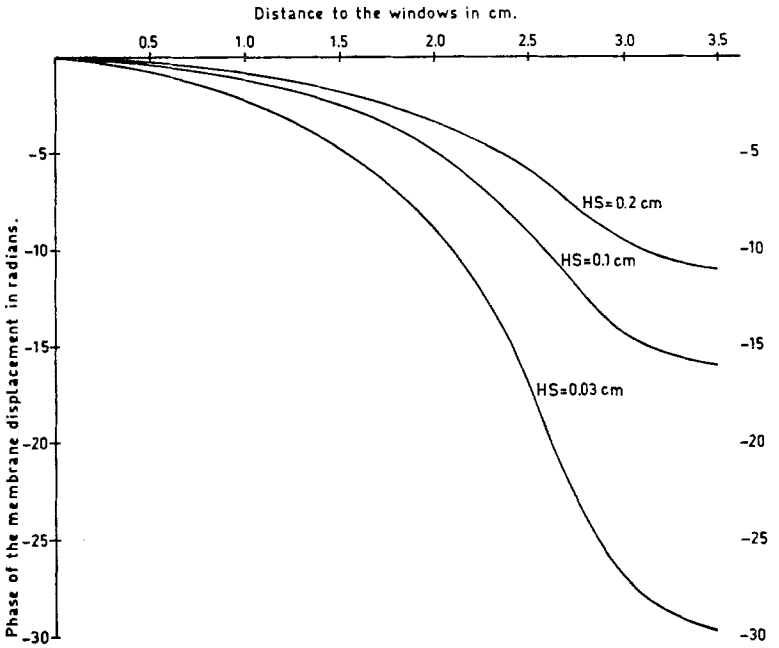

Figure 7. Phase of the membrane displacement $\eta(x)$ as a function of position along the membrane for various scalaheights (HS). The frequency of the input signal was 1 kHz. The phase was referenced to $\eta(0)$.

Another interesting point is the influence of the step-unit in the integration process. In the above calculations 0.02 cm was used, so that the membrane was divided into 175 sections. In Fig. 8 $|\eta(x)|$ is shown for various step-units $(3.5/N)$ and an input frequency of 1000 Hz. The case $N = 175$ was hardly discernable from $N = 350$. It appears that both the size of the maximum displacement and its distance to the basal end decrease with decreasing N. For small values of N moreover, the shape of the curve is affected.

In the foregoing all quantities were plotted as a function of distance to the basal end for a constant frequency of the input signal. In Fig. 9 the magnitude of the membrane displacement is shown as a function of frequency for constant positions on the membrane. For frequencies < 500 Hz the picture is obscure due to the standing waves that arise. For higher frequencies the displacement decreases in amplitude with a slope dependent on the position along the membrane. The decibel scale was used because of the large amplitude ratios involved.

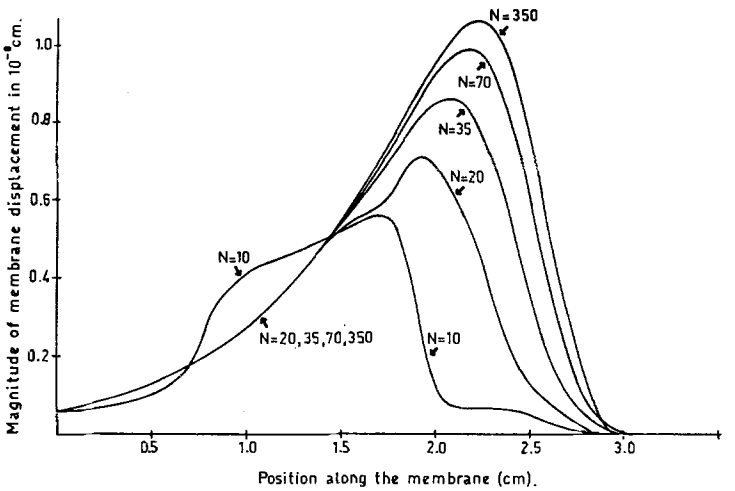

Figure 8. The magnitude of the basilar membrane displacement as a function of distance along the membrane for various numbers (N) of steps during the integration process. The frequency of the input signal was 1 kHz; the input transmembrane pressure $p(0)$ was 1 dyn/cm^2.

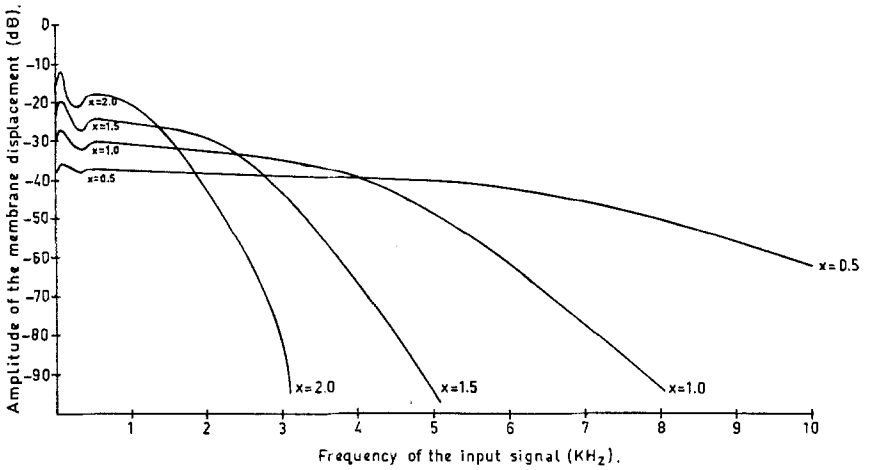

Figure 9. Amplitude of the membrane displacement as a function of frequency for several points on the membrane. 0 dB = 10^{-7} cm displacement when $p(0) = 1$ dyn/cm^2.

Fig. 10 presents the phase of the membrane displacement as a function of frequency. The most conspicious feature is that the phase lag does not increase monotonically but reaches a maximum; this lies in the range of hearing except for the basal end part of the partition.

Finally the phase velocity of the displacement wave is shown in Fig. 11 as a function of frequency. For frequencies < 100 Hz the phase velocity is large; this corresponds with Fig. 4 where was noticed that for these small frequencies the whole membrane practically moves in phase. When frequencies < 500 Hz are disregarded, the general picture of Fig. 11 is an almost constant phase velocity at first, slowly decreasing when the best frequency is

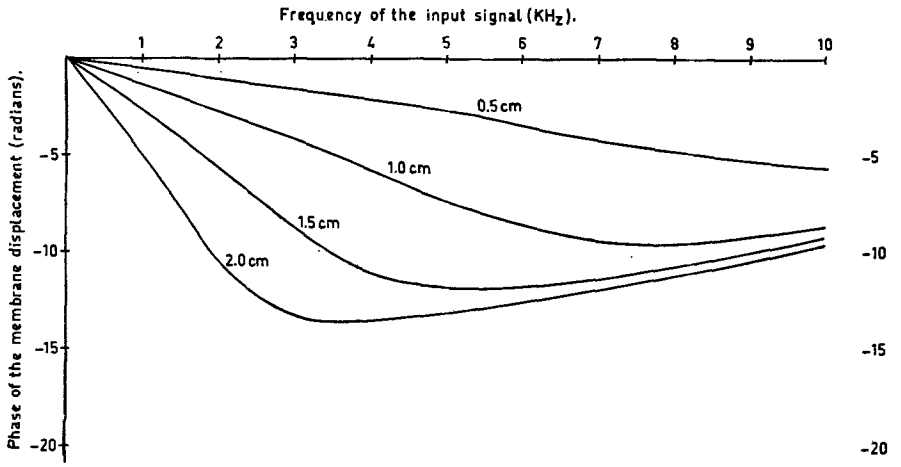

Figure 10. Phase of the membrane displacement as a function of frequency for several points on the membrane. The phase was referenced to its value at $x = 0$.

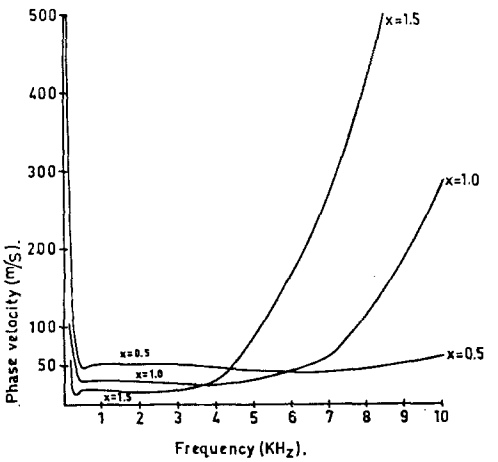

Figure 11. The phase velocity of the membrane displacement wave as a function of frequency for various positions on the membrane.

approached, increasing thereafter, at first slowly, then fast. For $x = 0.5$ cm, the best frequency is about 6 kHz, as can be seen in Fig. 3; for $x = 1.0$ cm and $x = 1.5$ cm, the best frequencies are 4 and 2 kHz respectively.

5. Discussion and conclusions

In this work a mathematically simple method has been developed to describe the two-dimensional model for the cochlea. The result for the simplest form of the model (incompressible and inviscid fluid; constant scala heights) is equation (2.14), which is approximated well by eq. (2.19). Moreover, the boundary conditions (2.20) and (2.26) are found which

can be derived directly from the conditions of the two-dimensional model. The results match completely with those in [12].

In Section 3 the compressibility of the fluid was taken into account. The resulting equation is (3.8), again with boundary conditions (2.20) and (2.26). Since the boundary conditions are identical to those in the incompressible case, the difference between (2.19) and (3.8) viz. the second term of (3.8) must account for the compressibility effects.

The numerical values given for $\zeta(x)$ in the literature show large differences, so that the frequency region for which the fluid is incompressible cannot be determined exactly. Yet it is clear that the role of the compressibility as to the results of the membrane displacement can only be a minor one in the frequency range of hearing, and certainly is negligible as compared to the inaccuracy of the numerical data.

Reckoning with the variation of the scala heights in the axial direction one obtains equation (3.11) which is approximated by (3.12). The appropriate boundary conditions for (3.12) are (2.20) and (3.13). The effect of the variations in $h(x)$ upon the boundary condition at the windows is presumably very small, but the effect upon the differential equation itself can be considerable. To my opinion, however, this extension has more theoretical than practical value, first because of the crudeness of the data on $h(x)$, second since in the model the scala heights are still taken as equal. With regard to the results of Section 4 an important remark must be made. The numerical values of $\zeta(x)$ and h are actually incompatible. Peterson and Bogert [5] used a scala cross section of $0.029 - 0.005x$ cm^2 and a membrane width of $0.019 + 0.0093x$ cm; consequently the scala height varies from 1.5 cm at the windows to 0.2 cm at the helicotrema. In reality, however, h varies from 0.2 cm to 0.05 cm, see [14]. The discrepancy stems from the one-dimensional nature of the Peterson–Bogert model, which does not allow a distinction between the membrane like part and the bony part of the cochlear partition. In the two-dimensional model such a discrepancy does not occur, since no uniformity of all quantities over a scala cross-section is required.

Because the correct value of h has to be used in the two-dimensional model, the probable consequence is that the value of ζ needs modification. Yet the values given by Peterson–Bogert were used, since the scope of this work was to acquire some qualitative conclusions only.

The results plotted in Figs. 2–4 show increasing differences between the one- and two-dimensional models with increasing frequency, as could be expected from the nature of the correction terms; for, $|\zeta|$ decreases with increasing frequency. In despite of the sometimes large quantitative differences, any qualitative disparities are hardly distinguishable.

Figs. 5–7 give the answer to an interesting question, namely whether the scala height bears some importance as to the motion of the partition.

Von Békésy [1] concluded from his model tests that the scala height could be extended to infinity without influencing the wave pattern of the partition, whereas a reduction of the scala height to 0.3 mm would cause a slight shift of the region of maximum excitation towards the basal end.

Fig. 6 shows that the latter conclusion is correct, but from both Figs. 6 and 7 it appears that the former is incorrect. It is true that the position of the maximum does not change when the scala height is increased, but the shape of the amplitude curve is affected and moreover the phase lag is reduced considerably. Further it is apparent that a reduction of the scala height brings about larger phase differences.

An indication of the effects of discretization in the axial direction can be gathered from Fig. 8. It is obvious that a 35 section model gives maximum displacements that are both too small and too close to the basal end. Therefore a hybrid computer model as presented by Hubbard and Geisler [4] is inaccurate, since it is confined to 31 sections. A 175-section model (Bogert, [2]) and a 100-section model (Wansdronk, [13]) give no significant deviations. The minimum number of sections is a matter of desired accuracy; for the purpose of this work 175 sections were good enough.

The results presented in Figs. 9 and 10 invite to an interesting discussion. The qualitative agreement of Fig. 10 with the experiments of Rhode [6] is excellent, since the latter were performed roughly 0.9 cm from the stapes. The quantitative agreement, however, is poor, since the measured phase lags were much larger than the calculated ones. The same holds for the amplitude. When the amplitude of the membrane displacement is divided by that of the stapes displacement, a curve is obtained that resembles that of Rhode; this was shown by Hubbard and Geisler [4] for the one-dimensional model. In the present model the discrepancies can be eliminated by taking a much smaller value for h (0.2 mm instead of 1 mm). Then the qualitative agreement is retained, but also good quantitative agreement is found. The argument becomes more interesting because Rhode performed his experiments by making a hole in the scala tympani. The effect of this is uncertain. To my opinion the more detailed representation of the cochlear partition as indicated by Steele [8] provides a more realistic explanation for the large phase lag, but the thought that an explanation is possible even with the simple point impedance characterization of the partition is appealing.

The phase velocity has been calculated to see whether the present model, being neither a long-wave nor a short-wave model, suffers from the main difficulty of all short wave models: a phase velocity that is inversely proportional to sound frequency (see [15]). The empirical evidence gives another picture (see e.g. [6]). From Fig. 11 it appears that the results are in qualitative agreement with the experiments of Rhode [6]; quantitative agreement can be obtained again by lowering the scala height considerably.

It is obvious that the results from our model are much better than those of the short-wave cochlear model of Siebert [7]. This, however, is not necessarily due to the short-wave character of that model, since Siebert obscured the singular character of the problem as noted by Van Dijk [3].

Acknowledgements

I wish to express my thanks to Mr. J. J. Kalker for his support in this investigation and for his critical reading of the manuscript, to Messrs. A. J. Hermans and A. H. P. van der Burgh for valuable discussions, and to Mr. G. Broere for his excellent drawings.

REFERENCES

[1] G. von Békésy, *Experiments in hearing*, McGraw Hill Book Company Inc., New York (1960).

[2] B. P. Bogert, Determination of the effects of dissipation in the cochlear partition by means of a network representing the basilar membrane, *J. Acoust. Soc. Am.* 23 (1951) 151–154.

[3] J. S. C. van Dijk, On the hydrodynamics of the inner ear. Theoretical part. A mathematical model, to appear in *Acustica*.

[4] A. E. Hubbard and C. D. Geisler, A hybrid computer model of the cochlear partition, *J. Acoust. Soc. Am.* 51 (1972) 1895–1903.
[5] L. C. Peterson and B. P. Bogert, A dynamical theory of the cochlea, *J. Acoust. Soc. Am.* 22 (1950) 369–381.
[6] W. S. Rhode, Observations of the vibration of the basilar membrane in squirrel monkeys using the Mössbauer technique, *J. Acoust. Soc. Am.* 49 (1971) 1218–1231.
[7] W. M. Siebert, Ranke revisited—a simple short wave cochlear model, *J. Acoust. Soc. Am.* 56 (1974) 594–600.
[8] C. R. Steele, Behavior of the basilar membrane with pure-tone excitation. *J. Acoust. Soc. Am.* 55 (1974) 148–162.
[9] M. A. Viergever, Non-linearities within the perilymph, *Delft Progress Report, Series F*, 1 (1974) 29–36.
[10] M. A. Viergever and J. J. Kalker, On the adequacy of the Peterson–Bogert model and on the effects of viscosity in cochlear dynamics, *J. Eng. Math.* 8 (1974) 149–156.
[11] M. A. Viergever and J. J. Kalker, Localization of non-linearities in the cochlea, *J. Eng. Math.* 9 (1975) 11–20.
[12] M. A. Viergever and J. J. Kalker, A two-dimensional model for the cochlea. I: The exact approach, *J. Eng. Math.* 9 (1975) 353–365.
[13] C. Wansdronk, *On the mechanism of hearing*, dissertation Leiden (1961).
[14] J. Zwislocki–Mościcki, Theorie der Scheckenmechanik, *Acta Oto-Laryngo logica, Suppl. LXXII*, Solothurn (1948).
[15] J. Zwislocki, Cochlear waves: their analysis and simulation on a transmission line, in *Physiology of the auditory system*, M. B. Sachs (Ed.), National Educational Consultants, Baltimore (1971).